From Yellow to Black: New Semiconducting Ba Chalcogeno-Germanates

Abdeljalil Assoud, Navid Soheilnia, and Holger Kleinke

Department of Chemistry, University of Waterloo, Waterloo, Ontario, Canada N2L 3G1

Reprint requests to Prof. Dr. H. Kleinke. E-mail: kleinke@uwaterloo.ca

Z. Naturforsch. **59b,** 975 – 979 (2004); received June 30, 2004

Dedicated to Professor Kurt O. Klepp on the occasion of his 60th birthday

The new germanates $Ba_2GeSe_{4-\delta}Te_\delta$ ($\delta < 2.5$) were prepared by reacting the elements under exclusion of air at 800 °C, followed by slow cooling to room temperature. These germanates form the Sr_2GeS_4 type, monoclinic space group $P2_1/m$, with lattice dimensions of $a = 699.58(4)$, $b = 709.38(4)$, $c = 917.38(6)$ pm, $\beta = 109.135(1)°$, $V = 430.11(4) \cdot 10^6$ pm^3 ($Z = 2$) for Ba_2GeSe_4. The structure contains isolated $GeSe_4$ tetrahedra. The oxidation states are assigned to be Ba^{II}, Ge^{IV}, and Se^{-II}. The yellow color of this ortho-seleno-germanate is indicative of semiconducting behavior with an activation energy of 2.6 – 3.0 eV, and the black appearance of the seleno-telluro-germanates points towards gaps < 1.7 eV. Electronic structure calculations based on the LMTO approximation resulted in smaller gaps of 1.7 – 0.8 eV, a tendency that is typical for this calculation method.

Key words: Electronic Structure, Semiconductor, Germanium, Selenium, Tellurium

Introduction

Research in thermoelectrics has led to quite significant improvements in the properties of new materials in recent years [1 – 5]. Thermoelectric materials often form complex yet highly symmetric crystal structures comprising heavy constituent elements [6, 7]. The ideal material ought to be a small band gap semiconductor with a gap in the range of $6 - 10\ k_BT$, with k_B = Boltzmann constant, and T = operating temperature [8]. This range corresponds to band gaps between 0.16 eV at 300 K and 0.7 eV at 800 K. The commercially used so-called TAGS family is a tellurogermanate, $(AgSbTe_2)_{1-x}(GeTe)_x$ [9, 10].

Most recently, we published on a new selenogermanate, $Ba_4LaSbGe_3Se_{13}$, a red semiconductor with a computed gap of 1.5 eV, whose structure comprises both $GeSe_4$ tetrahedra and Ge_2Se_7 double tetrahedra [11]. A few ternary and higher selenogermanates-(IV) were known prior to our investigation, including Sr_2GeSe_4 [12], $KLaGeSe_4$ [13], and $K_2Hg_3Ge_2Se_8$ [14]. The here-with introduced new seleno- and seleno-telluro-germanates crystallize in the Sr_2GeS_4 [15] type, isostructural with the corresponding chalcogeno-silicates Ba_2SiSe_4 and Ba_2SiTe_4 [16]. While Scifinder Scholar reveals Registry Numbers for Ba_2GeSe_4 (216600-10-1) and "Ba_2GeTe_4" (216601-36-4), this information is misleading, for it was erroneously extracted from a European Patent Application that does not mention these compounds [17].

Experimental Section

Synthesis and analysis

All synthesis attempts started from the elements as acquired from ALDRICH and ALFA AESAR, with nominal purities above 99%. The elements Ba, Ge, and Se were loaded in the 2 : 1 : 4 stoichiometric ratio into a silica tube, which was subsequently evacuated and then sealed to achieve exclusion of air. The fused silica tubes were placed into a programmable resistance furnace, which was heated to 800 °C, kept at that temperature for a period of five days, and then slowly cooled down to room temperature (with 1 °C/h). X-ray powder diffractograms obtained from the ground sample, utilizing the INEL powder diffractometer with a position-sensitive detector (Cu-K_α radiation), revealed the absence of any known materials. After the crystal structure determination (described below) proved the successful synthesis of the target compound, Ba_2GeSe_4, we simulated its powder diagram based on the refined structural parameters. A comparison of this diagram with the experimentally obtained one showed quantitative yields of Ba_2GeSe_4.

To determine whether Se in Ba_2GeSe_4 can be replaced by Te, we carried out a set of reactions with the starting ratio of 2 Ba : 1 Ge : $(4 - \delta)$ Se : δ Te, with $\delta = 2$, 3, and 4. Only in

Table 1. Crystallographic data of $Ba_2GeSe_{4-\delta}Te_\delta$.

Chemical formula	Ba_2GeSe_4	$Ba_2GeSe_2Te_2$	$Ba_2GeSe_{1.53(1)}Te_{2.47}$
Formula weight [g/mol]	663.11	760.39	783.25
T [K], λ [pm] of measurement	298, 71.073	298, 71.073	298, 71.073
Crystal size [μm]	80×40×20	90×45×20	100×50×20
Space group, Z	$P2_1/m$, 2	$P2_1/m$, 2	$P2_1/m$, 2
a [pm]	699.58(4)	732.12(8)	745.87(6)
b [pm]	709.38(4)	719.09(8)	731.63(6)
c [pm]	917.38(6)	928.5(1)	937.15(8)
β [°]	109.135(1)	108.433(2)	108.429(2)
V [10^6 pm^3]	430.11(4)	463.75(9)	485.18(7)
μ [mm^{-1}]	29.350	25.539	24.034
$F(000)$	560	632	649
ρ_{calcd} [g/cm^3]	5.120	5.445	5.361
Goof on F^2	1.086	1.083	1.152
$R(F_o)$;	0.0261;	0.0479;	0.0399;
$R_w(F_o^2)(I > 2(I))$	0.0581	0.1070	0.0859
$R(F_o)$;	0.0286;	0.0565;	0.0488;
$R_w(F_o^2)$ (all data)	0.0594	0.1111	0.0896
Extinction coeff.	0.0082(4)	0.0002(2)	0.0003(2)
Effective min. transmission	0.62	0.66	0.67
Largest diff. peak; hole [e/Å^3]	1.35; −1.24	2.71; −2.92	2.40; −1.40

Table 2. Atomic coordinates and equivalent displacement parameters of Ba_2GeSe_4.

Atom	Wyckoff notation	x	y	z	U_{eq} [Å^2]
Ba1	2e	0.21266(4)	1/4	0.54580(3)	0.01445(7)
Ba2	2e	0.28540(4)	1/4	0.07688(3)	0.01569(7)
Ge	2e	0.79291(7)	1/4	0.71097(5)	0.01046(9)
Se1	2e	0.63161(8)	1/4	0.44204(5)	0.0195(1)
Se2	2e	0.58570(8)	1/4	0.86643(5)	0.0186(1)
Se3	4f	0.98951(5)	0.49117(4)	0.22706(4)	0.01345(8)

the first case, phase pure $Ba_2Ge(Se/Te)_4$ was achieved, which implies that between two and three Se atoms per formula unit of Ba_2GeSe_4 may be replaced with Te atoms. Standardless Energy Dispersive Spectroscopy (EDS, LEO 1050) indicated the absence of any impurities of other elements (like silicon or oxygen stemming from the silica tube), and pointed towards a homogeneous Se/Te distribution throughout that sample.

Single crystal data were collected on crystals taken from the reaction excluding Te (yellow crystal), from the reaction with a Se : Te ratio of 2 : 2 (black crystal), and from the reaction with a Se : Te ratio of 1 : 3 (black crystal). All data collections were carried out on a BRUKER Smart Apex CCD at room temperature, utilizing graphite-monochromatized Mo-$K_{\alpha 1}$ radiation (crystal-to-detector distance: 4.550 cm). Scans of 0.3° in ω were performed in two groups of 606 frames at $\phi = 0°$ and 60° in each of the three cases. The data were corrected for Lorentz and polarization effects. Absorption corrections were based on fitting a function to the empirical transmission surface as sampled by multiple equivalent measurements using SADABS [18].

Table 3. Atomic coordinates and equivalent displacement parameters of $Ba_2GeSe_2Te_2$.

Atom	Wyckoff notation	x	y	z	U_{eq} [Å^2]
Ba1	2e	0.2146(1)	1/4	0.55179(9)	0.0169(2)
Ba2	2e	0.2444(2)	1/4	0.0605(1)	0.0220(2)
Ge	2e	0.7862(2)	1/4	0.7041(2)	0.0141(3)
Te1	2e	0.6210(2)	1/4	0.4184(1)	0.0234(3)
Te2	2e	0.5979(2)	1/4	0.8868(1)	0.0311(3)
Se3	4f	0.0021(2)	0.4951(1)	0.2396(1)	0.0168(2)

Table 4. Atomic coordinates and equivalent displacement parameters of $Ba_2GeSe_{1.5}Te_{2.5}$.

Atom	Wyckoff notation	x	y	z	U_{eq} [Å^2]
Ba1	2e	0.21969(6)	1/4	0.55394(5)	0.0206(1)
Ba2	2e	0.23869(7)	1/4	0.05989(5)	0.0239(1)
Ge	2e	0.78527(9)	1/4	0.70008(8)	0.0147(2)
Te1	2e	0.61479(7)	1/4	0.41553(5)	0.0242(1)
Te2	2e	0.60213(7)	1/4	0.89052(5)	0.0255(1)
0.765(6) Se, 0.235 Te	4f	0.99995(6)	0.49390(6)	0.24260(5)	0.0193(2)

The systematic absences and the lattice cell dimensions pointed towards formation of the Sr_2GeS_4 type, space group $P2_1/m$. We used the atomic positions published for isostructural Ba_2SiSe_4 as the starting model, assigning Ge to the original Si site. The refinements [19] converged smoothly to satisfactory residual values and unsuspicous displacement parameters. In case of the seleno-telluro-germanates, we allowed for mixed occupancies on all chalcogen sites. The refinements revealed a high tendency to Se/Te ordering, as only one out of three chalcogen sites (Q3) turned out to be mixed occupied in the most Te-rich sample, while complete Se/Te ordering was found in the sample with a Se : Te starting ratio of 2 : 2, resulting in the formula $Ba_2GeSe_2Te_2$. In the former case, the refined formula is $Ba_2GeSe_{1.53(1)}Te_{2.47}$, which is likely to represent the most Te-rich phase of the $Ba_2GeSe_{4-\delta}Te_\delta$ series. Hence, the phase range covers at least $0 \leq \delta \leq 2.47$. Subsequently we synthesized pure $Ba_2GeSe_{1.5}Te_{2.5}$ by starting from the elements in the stoichiometric ratio of 2 : 1 : 1.5 : 2.5 under the same conditions as described above for Ba_2GeSe_4.

Crystallographic details are given in Table 1, atomic positions and equivalent displacement parameters in Tables 2 – 4. Further details of the crystal structure investigations can be obtained from the Fachinformationszentrum Karlsruhe, 76344 Eggenstein-Leopoldshafen, Germany, (fax: (49) 7247-808-666; e-mail: crysdata@fiz-karlsruhe.de) on quoting the depository numbers CSD-414164, CSD-414165 and CSD-414166.

Attempted conductivity measurements: Two phase-pure Te-containing samples of nominal composition $Ba_2GeSe_2Te_2$ and $Ba_2GeSe_{1.5}Te_{2.5}$ were thoroughly

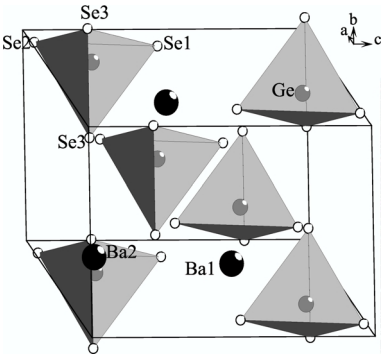

Fig. 1. Structure of Ba_2GeSe_4 in a projection along [100]. Black circles: Ba; gray: Ge; white: Se. $GeSe_4$ tetrahedra are shown as gray polyhedra. Ba−Se bonds are omitted for clarity.

ground, and then pressed into two bar-shaped pellets of the dimensions $6 \times 1 \times 1$ [in mm]. The high resistance of the pellets inhibited Seebeck and electrical conductivity measurements. We conclude based on our experiences with other high resistance materials that their specific resistances must be above 100 KΩcm at room temperature.

Electronic structure calculations: The self-consistent tight-binding *first principles* LMTO method (LMTO = Linear Muffin Tin Orbitals) was utilized using the atomic spheres approximation (ASA) [20, 21]. In the LMTO approach, the density functional theory is used with the local density approximation (LDA) [22]. The integration in *k* space was performed by an improved tetrahedron method [23] on a grid of 2222 independent *k* points of the first Brillouin zone of Ba_2GeSe_4 and $Ba_2GeSe_2Te_2$. The ASA radii of the Se atoms in Ba_2GeSe_4 are 139 pm for Se1, 138 pm for Se2, and 136 pm for Se3. For the case of $Ba_2GeSe_{1.5}Te_{2.5}$, where one position (Q3) with a multiplicity of four is mixed occupied by 76.5(6)% Se and 23.5% Te, we developed an ordered model to simulate its electronic structure. We chose the simplest model, based on the same unit cell with space group *P*1, that yielded four symmetry independent sites corresponding to the original Q3 position (Wyckoff notation 4f). We assigned one Te atom and three Se atoms to these four independent sites, hence simulating a 75% Se occupancy instead of the refined 76.5(6)%. The resulting stochiometry is $Ba_2GeSe_{1.5}Te_{2.5}$, and a grid of 800 *k* points was used in this case.

Results and Discussion

Crystal structure and bonding

Ba_2GeSe_4 crystallizes in the Sr_2GeS_4 type, isostructural with Ba_2SiSe_4. We were unable to synthesize the ternary Ba telluro-germanate Ba_2GeTe_4, whereas Ba_2SiTe_4 was reported to be isotypic with Ba_2SiSe_4. $Ba_2GeSe_2Te_2$ is an ordered ternary variant, which has two chalcogen atom sites filled exclusively with Te, and one with Se (Q3). The latter is the smallest Se site in Ba_2GeSe_4, as *e.g.* verified by the ASA radius of 136 pm for Se3, compared to radii of 139 and 138 pm for Se1 and Se2. Up to (at least) 25% of this site may be occupied by Te, resulting in the most Te-rich compound of the series, $Ba_2GeSe_{1.5}Te_{2.5}$ found to date.

Table 5. Selected interatomic distances [pm].

Bond	no.	Ba_2GeSe_4	$Ba_2GeSe_2Te_2$	$Ba_2GeSe_{1.5}Te_{2.5}$
Ba1-Q1		336.53(6)	356.6(2)	357.55(7)
Ba1-Q1	2×	370.14(3)	377.38(6)	384.25(3)
Ba1-Q1		385.9(1)	412.5(2)	428.2(3)
Ba1-Q2		322.96(6)	346.9(2)	352.10(7)
Ba1-Q3	2×	330.47(4)	332.9(1)	337.05(6)
Ba1-Q3	2×	341.26(4)	340.2(1)	343.58(6)
Ba2-Q1		343.06(6)	358.5(1)	361.47(7)
Ba2-Q2		328.63(6)	345.5(2)	354.80(7)
Ba2-Q2	2×	365.47(2)	376.06(6)	382.87(4)
Ba2-Q3	2×	331.35(4)	329.9(1)	334.89(6)
Ba2-Q3	2×	336.58(4)	334.6(1)	339.48(6)
Ge-Q1		235.26(6)	254.4(2)	256.60(8)
Ge-Q2		234.32(7)	250.2(2)	256.76(9)
Ge-Q3	2×	233.32(5)	235.0(1)	241.28(6)

These compounds can be classified as orthogermanates, for only discrete (more or less regular) $Ge^{IV}Q_4$ tetrahedra (Q = Se, Te) exist in this structure (Fig. 1). The same is true for the structures of the isoelectronic but not isostructural compounds Ba_2SiS_4 and Ba_2GeS_4 (β-K_2SO_4 type) [24]. Schäfer *et al.* [16] showed that these compounds nicely fit (more or less) into a structure map based on the radii of the A and B atoms of A_2BQ_4 (with Q = S, Se, Te). However, since r_A and r_B are constants in the Ba_2SiQ_4 series, one would expect Ba_2SiS_4 and Ba_2SiSe_4 to be isostructural – which they are not. Similarly, Ba_2GeS_4 and Ba_2GeSe_4 are not isostructural, indicating that the different chalcogen atoms cannot be ignored in such structure predictions. A more complex concept includes electronegativies as well as the radii of the Q atoms, but this has not yet been expanded to include selenides and tellurides [25].

Table 5 compares the interatomic distances of Ba_2GeSe_4, $Ba_2GeSe_2Te_2$, and $Ba_2GeSe_{1.5}Te_{2.5}$. In Ba_2GeSe_4, the Ge−Se bonds range from 233 to 235 pm (with the Ge−Se3 bond being the shortest). This compares well to the bonds in the binary selenide α-$GeSe_2$ (234 – 237 pm [26]). The list of the bond angles, which vary from 104° to 117° (Ta-

Table 6. Selected bond angles [°].

Bond angle	no.	Ba_2GeSe_4	$Ba_2GeSe_2Te_2$	$Ba_2GeSe_{1.5}Te_{2.5}$
Q1-Ge-Q2		117.29(3)	121.66(7)	121.64(3)
Q1-Ge-Q3	2×	107.809(17)	107.15(5)	107.90(2)
Q2-Ge-Q3	2×	109.635(17)	108.36(5)	107.87(2)
Q3-Ge-Q3		103.80(3)	102.53(7)	101.89(3)

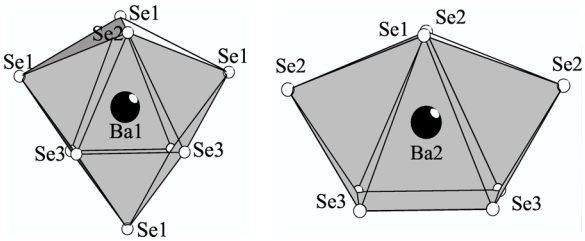

Fig. 2. $Ba1Se_9$ and $Ba2Se_8$ polyhedra of Ba_2GeSe_4.

ble 6), reveals only small deviations from ideal tetrahedral symmetry. As expected, the Ge−Te distances are significantly larger (250 – 257 pm), and correspondingly the Ge−Q3 bond is increased to 241 pm in $Ba_2GeSe_{1.5}Te_{2.5}$, when the Q3 site contains 25% Te.

As shown in Fig. 2, the two crystallographically independent Ba sites exhibit coordination numbers of nine (Ba1) and eight (Ba2). The respective coordination polyhedra may be described as tri- and bi-capped trigonal prisms, where the Ba−Q distances to the capping Q sites are significantly larger than to the six corners of the prisms. For Ba1 in Ba_2GeSe_4, the distances to the capping positions (Se1) are 2×370 pm and 1×386 pm, compared to the distances to the corners of 330 - 341 pm. Similarly, the distances for Ba2 are 2×366 pm to the capping Se2 sites, and between 329 and 343 pm to the vertices of the trigonal prism. Hence, one may describe the coordination numbers as $6+3$ for Ba1 and $6+2$ for Ba2. That Se3 exclusively occupies the vertices supports the observed preference of the Te atoms for the other two Q sites: each Se3 atom participates in four Ba−Se bonds below 350 pm, compared to two for Se1 and two for Se2. Somewhat smaller Ba−Se distances were found in Ba_2SiSe_4, ranging from 321 to 369 pm for Ba1, and from 331 to 361 pm for Ba2.

Electronic structure and physical properties

The yellow appearance of Ba_2GeSe_4 is indicative of a band gap of 2.6 – 3.0 eV [27]. The calculated Densities of States (left part of Fig. 3) reveal a gap between empty Ge-*s* states and filled Se-*p* states of 1.7 eV, *i.e.* 35% smaller than expected. Such a discrepancy is not atypical for local density approximations [11, 28, 29]. The calculations show the right tendency, however, as the gaps for the quaternary (ordered) variants $Ba_2GeSe_2Te_2$ (1.0 eV) and $Ba_2GeSe_{1.5}Te_{2.5}$ (0.7 eV) are in the range of black semiconductors (< 1.7 eV), and black appearance was observed for both cases. The decreasing size of the gap with increasing Te content is caused by the lower ionization potential of Te, compared to Se, leading to a shift of the chalcogen *p*-block towards the Ge-*s* states, as well as a broadening of the chalcogen states.

Taken the tendency of underestimating the gap size into consideration, it can be concluded that the band gap of the most Te-rich phase, $Ba_2GeSe_{1.5}Te_{2.5}$, lies

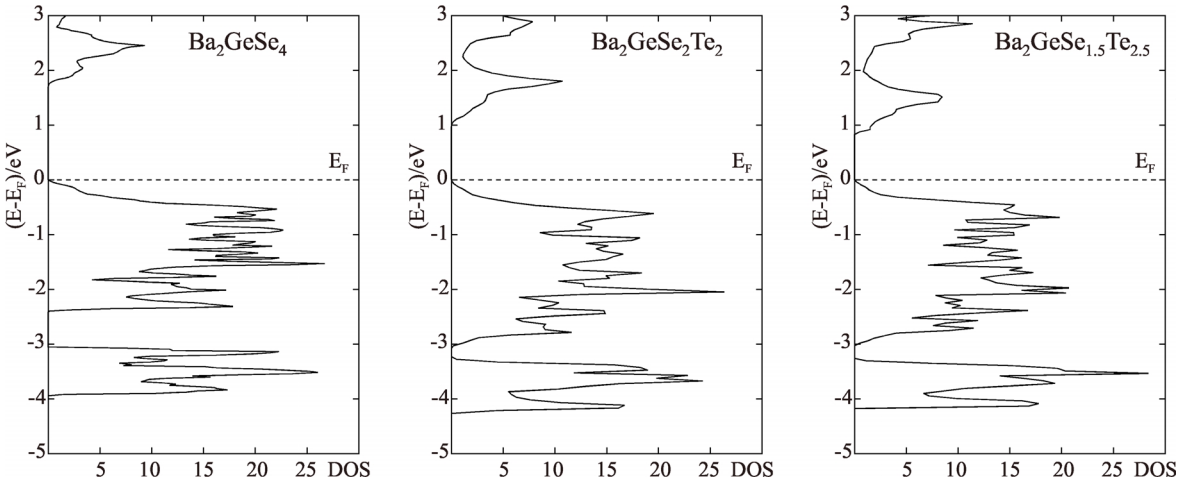

Fig. 3. Densities-Of-States (DOS) for Ba_2GeSe_4 (left), $Ba_2GeSe_2Te_2$ (center) and the $Ba_2GeSe_{1.5}Te_{2.5}$ model (right). The Fermi level, E_F, (dashed line) was arbitrarily placed at 0 eV.

between 0.8 and 1.1 eV. This is still too large for the thermoelectric energy conversion [8]. Undoped semiconductors with such gaps have too high electrical specific resistances, as our own measurements for $Ba_2GeSe_2Te_2$ and $Ba_2GeSe_{1.5}Te_{2.5}$ confirmed.

Summary

We present a new Ba seleno-germanate, Ba_2GeSe_4, and its isotypic quaternary ordered variants $Ba_2GeSe_2Te_2$ and $Ba_2GeSe_{1.5}Te_{2.5}$. Ba_2GeSe_4 is an ortho-germanate crystallizing in the Sr_2GeS_4 type. The Te site preferences can be understood based on size effects, and on the Ba coordination in particular.

Replacing Se in part with Te leads to a decrease in the band gap size, as reflected in the change from the yellow color of Ba_2GeSe_4 to the black appearance of both $Ba_2GeSe_2Te_2$ and $Ba_2GeSe_{1.5}Te_{2.5}$. This trend could be verified *via* LMTO-based band structure calculations. Still, the electrical resistivities of all samples are too high to be measured.

Acknowledgements

Financial support from NSERC, CFI, OIT (Ontario Distinguished Researcher Award for H. K.), the Province of Ontario (Premier's Research Excellence Award for H. K.) and the Canada Research Chair program (CRC for H. K.) is appreciated.

[1] B. C. Sales, D. Mandrus, R. K. Williams, Science (Washington, D. C.) **272**, 1325 (1996).
[2] D.-Y. Chung, T. Hogan, P. Brazis, M. Rocci-Lane, C. Kannewurf, M. Bastea, C. Uher, M. G. Kanatzidis, Science (Washington, D. C.) **287**, 1024 (2000).
[3] R. Venkatasubramanian, E. Slivola, T. Colpitts, B. O'Quinn, Nature (London) **413**, 597 (2001).
[4] K. F. Hsu, S. Loo, F. Guo, W. Chen, J. S. Dyck, C. Uher, T. Hogan, E. K. Polychroniadis, M. G. Kanatzidis, Science (Washington, D. C.) **303**, 818 (2004).
[5] D.-Y. Chung, T. P. Hogan, M. Rocci-Lane, P. Brazis, J. R. Ireland, C. R. Kannewurf, M. Bastea, C. Uher, M. G. Kanatzidis, J. Am. Chem. Soc. **126**, 6414 (2004).
[6] D. M. Rowe, CRC Handbook of Thermoelectrics, CRC Press, Boca Raton, FL, 1995.
[7] F. J. DiSalvo, Science (Washington, D.C.) **285**, 703 (1999).
[8] J. O. Sofo, G. D. Mahan, Phys. Rev. **B49**, 4565 (1994).
[9] E. A. Skrabek, D. S. Trimmer, in D. M. Rowe (ed.): CRC Handbook of Thermoelectrics, p. 267, CRC Press, Boca Raton, FL (1995).
[10] L. E. Shelimova, P. P. Konstantinov, O. G. Karpinsky, E. S. Avilov, M. A. Kretova, J. P. Fleurial, Intern. Conf. Thermoelectr. **18**, 536 (1999).
[11] A. Assoud, N. Soheilnia, H. Kleinke, J. Solid State Chem. **177**, 2249 (2004).
[12] R. Pocha, M. Tampier, R.-D. Hoffmann, B. D. Mosel, R. Pöttgen, D. Johrendt, Z. Anorg. Allg. Chem. **629**, 1379 (2003).
[13] P. Wu, J. A. Ibers, J. Solid State Chem. **107**, 347 (1993).
[14] X. Jin, L. Zhang, G. Shu, R. Wang, H. Guo, J. Alloys Comp. **347**, 67 (2002).
[15] E. Philippot, M. Ribes, M. Maurin, Rev. Chim. Mineral. **8**, 99 (1971).
[16] C. Brinkmann, B. Eisenmann, H. Schäfer, Z. Anorg. Allg. Chem. **524**, 83 (1985).
[17] T. Sato, Y. Bito, T. Murata, S. Ito, H. Matsuda, Y. Toyoguchi, in Eur. Pat. Appl., p. 37 pp., Matsushita Electric Industrial Co., Ltd., Japan. EP (1998).
[18] SAINT, Siemens Analytical X-ray Instruments Inc., Madison, WI. (1995).
[19] G. M. Sheldrick, SHELXTL, Siemens Analytical X-Ray Systems, Madison, WI. (1995).
[20] O. K. Andersen, Phys. Rev. **B12**, 3060 (1975).
[21] H. L. Skriver, The LMTO Method, Springer, Berlin, Germany (1984).
[22] L. Hedin, B. I. Lundqvist, J. Phys. **4C**, 2064 (1971).
[23] P. E. Blöchl, O. Jepsen, O. K. Andersen, Phys. Rev. **B49**, 16223 (1994).
[24] K. Susa, H. Steinfink, J. Solid State Chem. **3**, 75 (1971).
[25] K. Kugimiya, H. Steinfink, Inorg. Chem. **7**, 1762 (1968).
[26] G. Dittmar, H. Schäfer, Acta Crystallogr. **B32**, 2726 (1976).
[27] K. Nassau, The Physics and Chemistry of Color, John Wiley & Sons, Inc., New York City, NY, USA (2001).
[28] H. Yanagi, S.-I. Inoue, K. Ueda, H. Kawazoe, J. Appl. Phys. **88**, 4159 (2000).
[29] M. Tampier, D. Johrendt, Z. Anorg. Allg. Chem. **627**, 312 (2001).